Mon. Not. R. Astron. Soc. **000**, 000–000 (0000) Printed 11 July 2013 (MN LATEX style file v2.2)

A survey of gas and dust in $z > 2$ protoclusters [II]: the SEDs and gas-to-dust ratios in galaxies lying at $z = 2.84$ in the H1549+19 field

C. Ross,[1⋆] S. C. Chapman,[1] M. Gurwell,[2] M. Aravena,[3] A. W. Blain,[4] J. Geach,[5] R. J. Ivison,[6,7] N. Reddy,[8] Ian Smail, [9] C. C. Steidel,[10]

[1] *Dalhousie University, Coburg Road, Halifax, NS* [2] *Harvard-Smithsonian Center for Astrophysics, 60 Garden Street, Cambridge, MA 02138, USA*
[3] *Institute for Astronomy, University of Edinburgh, Royal Observatory, Blackford Hill, Edinburgh EH9 3HJ*
[4] *Joint ALMA Office, El Golf 40, Las Condes, Santiago 7550108, Chile*
[5] *UK Astronomy Technology Centre, Royal Observatory, Blackford Hill, Edinburgh EH9 3HJ*
London SW7 2BW, UK
[9] *Institute for Computational Cosmology, Durham University, South Road, Durham DH1 3LE*

DRAFT DATED: 11 JULY 2013

ABSTRACT

We present high-resolution interferometric imaging of the core regions of the protoclusters in the H1549+19 field ($z = 2.84$) and the H1700+64 field ($z = 2.30$). Our observations were made at ∼870 μm with the Submillimetre Array (SMA), following up deep SCUBA2 maps of these fields. Our high-resolution submm imaging detects 4 + XXX galaxies in continuum at $\gtrsim$4σ as single compact (size $\lesssim$2 arcsec or $\lesssim$16 kpc) point sources and yields absolute position to ∼0.4-arcsec accuracy. These sources are clearly associated to known CO(3-2) line emitters in the H1549 field, identified in our blind survey of this overdense region. At these redshifts, the 24μm–to–submm flux density ratios suggest that most of these protocluster galaxies have Arp 220-type starburst-dominated far-IR SED, while MD17 is more similar to XXX, with a more significant contribution at 24–μm (rest-frame $5-6$ μm) from an active nucleus. Gas-to-dust ratios are measured for all CO-emitters identified in the protocluster, with a median of 143 in solar units, and a dispersion of only 39, dominated by the outliers, MD17 and MD12. High apparent gas-to-dust ratio (> 150) can indicate the bulk of the dust mass is cold in some of the objects, while the tight gas-to-dust ratio found overall can be used to argue for a constant conversion between CO and H_2 gas mass. These CO and submm continuum maps in the core region of H1549 have helped to reveal how the large cold gas reservoirs, yet typical gas to dust ratios is likey driving the reversal in the SF-environmental density relation found in high$-z$ protoclusters (Ross et al. 2013). This complex mix of star–formation and AGN activity in multi–component sources may be common in the high redshift ultraluminous galaxy population, and highlights the need for precise astrometry from high resolution interferometric imaging for a more complete understanding.

Key words: galaxies: starburst – galaxies: formation – galaxies: high-redshift – cosmology: observations – submillimetre

1 INTRODUCTION

Measuring the evolution of molecular gas density is critical to understand the formation of stars in galaxies. For this, it is necessary to perform blind surveys of the sky that allow us to measure the molecular gas content in a CO flux limited sample as a function of redshift and luminosity (e.g. observations in the local Universe and simulations by Keres et al. 2003; Obreschkow & Rawlings 2009; Obreschkow et al. 2009; Lagos et al. 2011; Geach & Papadopolous 2012). Sensitive interferometers (e.g., SMA, PdBI, ALMA, CARMA) are making these studies possible.

Current observations and simulations suggest that there has been a strong evolution in the molecular gas fractions in star-forming disk galaxies at $z = 1-2$ compared to similar objects at $z < 0.5$ (Geach et al. 2009; Lagos et al. 2011; Aravena et al. 2012; Ross et al. 2013). However, the gas supplies, star formation efficiencies, and starburst modes (merger driven versus quiescent disk) may vary strongly as a function of their local density. Galaxy

⋆ E-mail: colin.ross@dal.ca

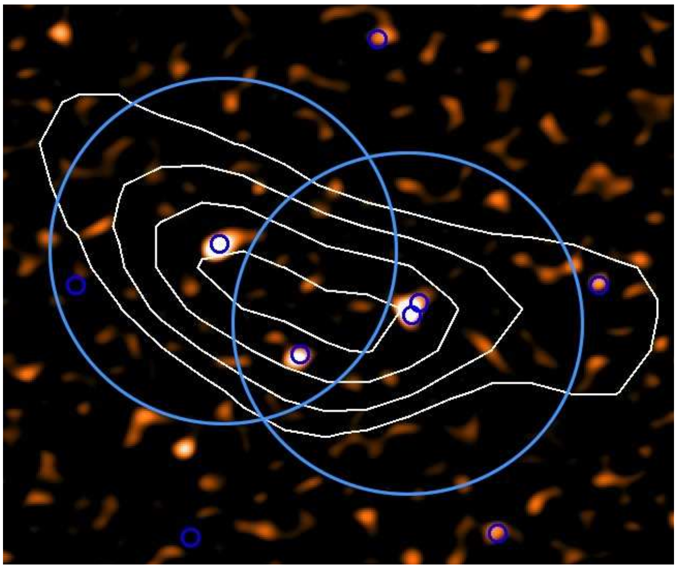

Figure 1. SMA 870μm map (40″ by 30″) of the $z\sim$2.84 H1549 protocluster field. CO-emitters from the PdBI map are shown as blue squares, while the SCUBA2 contours are shown overlaid (white). The SMA has effectively detected at least 5 of the CO emitters at 870μm continuum, clearly explaining the unresolved SCUBA2 emission, and allowing for far-IR SEDs to be fit to individual CO-emitting galaxies, and gas/dust ratios to be estimated precisely. We will constrain their ISM properties and elucidate the effect of the large overdensity on the gas supplies, stellar masses, and star formation modes relative to the field population.

evolution should be accelerated in regions of strong overdensity. Recent work with *Spitzer* and *Herschel* has demonstrated enhanced star formation rate (SFR), and reversal of the star formation(SF)-environmental density relation, at z>1.5 in galaxy clusters (Elbaz et al. 2007, 2011; Tran et al. 2011). Exceptionally high level of star formation have been found in cluster cores, reaching >2000 $M_\odot$/yr Mpc^{-2}. The reversal of the z<1 trend in SF vs environmental density implies that at $z\sim$2 massive cluster galaxies are still forming a substantial fraction of their stars in protoclusters. These high$-z$ protoclusters are where the morphology-density relation may be established.

We have initiated a project (the *Galaxy Overdensity Gas Survey*) to perform blind surveys of the gas and dust in $z > 2$ galaxy overdensities, or protoclusters, to provide a solid constraint on the evolving CO LF (Fig 1) in comparison with the field. An unique aspect of this program is the selection of the protoclusters from the 24 survey fields of the Keck Baryonic Structure Survey (KBSS; Rudie et al. 2012), a well calibrated field galaxy survey at $z > 2$. Several of these fields show strong galaxy overdensities (e.g., Steidel et al. 2000, 2005, 2010), providing a complete, unbiased census of protoclusters. H1549+19 (Figs. 2,3) contains the strongest KBSS overdensity (at $z\sim$2.84), with over 5 times the typical surface density of Lyman-α emitters (LAEs) found in the field. It is the richest LAE field ever observed, at any redshift.

In this paper, we present high-resolution SMA 870-μm interferometric imaging of H1549+19, the most overdense protocluster in KBSS. In § 2 we describe our observations and data reduction, and in § 3 we discuss some possible implications of our results. Throughout this paper, we use the Vega magnitude system, and assume a flat concordance cosmology with $(\Omega_{\rm m}, \Omega_\Lambda, {\rm H}_0) = (0.3, 0.7, 70\ {\rm km\,s^{-1}\,Mpc^{-1}})$.

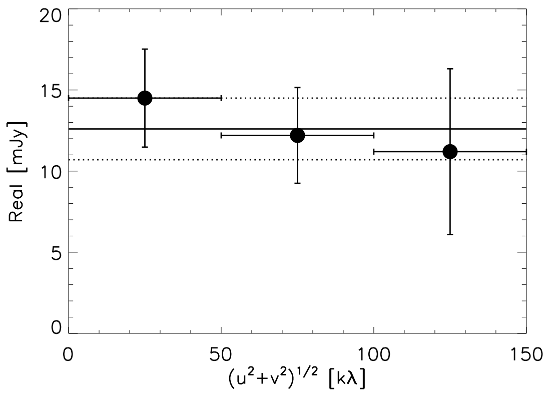

Figure 2. Visibilities of Q1549, showing the source is extended beyond the beam of SMA, with likely separation of $\sim 2''$. This is consistent with findings from Ross et al. (2013) that this source represents two CO(3-2) galaxies within the PdBI 3″ beam.

2 OBSERVATIONS AND DATA REDUCTION

NOTE: other $> 4\sigma$ detections in SMA map?? Nope.

The SMA observations were performed during 2007 March in the compact configuration (beam size $\sim$2 arcsec) in excellent weather ($\tau_{\rm 225GHz} \lesssim 0.08$) with a total on-source integration time of approximately 6 hr. The USB was tuned to 345 GHz, and combined with the LSB for an effective bandwidth of ~ 4 GHz at 340 GHz, which yielded a final synthesised image r.m.s. of 1.95 mJy. The pointing centre was the original SCUBA position from **?**: α(J2000) $= 10^{\rm h}52^{\rm m}57.32^{\rm s}$ and δ(J2000) $= +57^\circ21'05.8''$. The data were calibrated using the MIR software package (**?**), modified for the SMA. Passband calibration was done using 3C 84, 3C 111, and Callisto. The absolute flux scale was set using obser-

ID	RA/Dec	S870[a] [mJy]	S450[b] [mJy]	S24[c] [mJy]	S3mm[e] [mJy]	SCO[d] [Jy km/s]	z_{CO}	comments
q1549	< 0.04	0.72 ± 0.01						
md17	0.11 ± 0.01	0.29 ± 0.02						
d14	0.16 ± 0.01	0.44 ± 0.03						
q1549nbr	0.07 ± 0.03	0.55 ± 0.04						
md12	< 7.0	< 7.0						
x35μm	6.3 ± 0.18	6.6 ± 0.17						
nbxxμm	10.2 ± 2.3	9.8 ± 2.3						
x11	40.7 ± 5.6	52.4 ± 5.2						
c1	40.7 ± 5.6	52.4 ± 5.2						

Table 1. Properties of the galaxies detected as CO(3-2) emitters

Figure 3. SEDs and fits

vations of Callisto and is estimated to be accurate to better than 20%. Time-dependent complex gain calibration was done using 0958+655 (0.6 Jy, 21.8° away) and 0927+390 (1.8 Jy, 37.7° away). The calibrator 0958+655 was also calibrated independently using 0927+390 and used for empirical verification of the astrometric uncertainty and the angular size of the target. Positions and flux densities were derived from the calibrated visibilities using the MIRIAD (**?**) software package.

We detect LH 850.02 in the synthesized image at $\gtrsim 6\sigma$. The calibrated visibilities were best fit by a single point source (see Figures **??** and 3) with an integrated flux density of $S_{890\mu\mathrm{m}} = 12.8 \pm 2.0$ mJy at a position of $\alpha(\mathrm{J2000}) = 10^{\mathrm{h}}52^{\mathrm{m}}57.162^{\mathrm{s}}$ and $\delta(\mathrm{J2000}) = +57°21'07.97''$, which is offset from the original SCUBA position by 3.28 arcsec. The astrometric uncertainties are $\Delta\alpha = 0.24$ arcsec (0.20 arcsec systematic; 0.13 arcsec statistical) and $\Delta\delta = 0.22$ arcsec (0.19 arcsec systematic; 0.10 arcsec statistical), in agreement with the expectations of **?** and **?**.

3 DISCUSSION

The synthesised SMA image (see Figure 3) clearly shows a single point source within the SCUBA beam. As noted in § 2, this source is offset from the SCUBA centroid by 3.28 arcsec, as compared to the 1σ SCUBA positional uncertainty of 2.1 arcsec ($\sigma \sim 0.91\,\theta/(\mathrm{S/N})$, where θ is the SCUBA beam FWHM of 14 arcsec and S/N is the signal-to-noise ratio, corrected for flux boosting; **?**). The point-source fit to the visibility data ($S_{890\mu\mathrm{m}} = 12.8 \pm 2.0$ mJy) is perfectly consistent with the expectation from the deboosted SCUBA flux of $S_{850\mu\mathrm{m}} = 13.4 \pm 2.1$ mJy (13.1 ± 2.3 mJy when centered on the SMA position), assuming a reasonable range of spectral slopes and temperatures ($S_\nu \propto B_\nu(T)\nu^\beta$; $\beta \approx 1-2$, $T \approx 20-60$ K). This supports the compactness of the submm emission seen in the visibility function (see Figure **??**); virtually none of the flux seen in the SCUBA map has been resolved out.

In Figure 3, we present (from left to right) the SMA "dirty" map and the derived submm position overlaid on optical (R-band), IRAC 3.6-μm, MIPS 24-μm and VLA 1.4-GHz imaging data. The SMA image clearly singles out the weaker of the two candidate radio counterparts, and this is the one which is *not* associated with the bright 24-μm source[1]. This is consistent with the photometric redshift of LH850.02N if we assume a starburst–dominated mid-IR spectrum similar to local ultraluminous IR galaxies (ULIRGs; e.g. **??**), analogous $z \sim 2$ systems (e.g., **??**, Huang et al. 2008, in prep.), or other SMGs (**???**).

The SCUBA and SMA imaging data – including upper limits at the location of LH850.02S – are marginally consistent with the observed far–IR SEDs of two luminous starbursts at $z \sim 4$ (LH850.02N) and $z \sim 2$ (LH850.02S) respectively. However, SMA imaging in combination with optical/near–IR photometric redshifts for both sources favors a scenario in which the submm emission from LH 850.02 arises almost entirely from LH 850.02N and is not a blend of two lower-luminosity sources. This is consistent with the predicted rarity of SMGs arising from confusion (**?**). At these redshifts, their 24μm–to–submm ratios (see also **?**) suggest that LH 850.02N has an Arp 220-type starburst-dominated far-IR SED, while LH 850.02S has a Mrk 231-type far-IR SED with a significant contribution from a warmer dust component such as a warm starburst (OFRGs; **?**) or active nucleus. This is qualitatively similar to SMM J094303+4700 (**?**), in which only one of the two radio counterparts (H6: **?**) shows strong CO emission, which could be explained by AGN heating of the dust in the intrinsically CO poor radio source (H7). Therefore, LH 850.02 and, by analogy many other SMGs with multiple radio identifications, may be physically associated systems in which the SMG starburst phase is associated with a period of intense AGN activity (**???**).

Furthermore, although the relatively low S/N ($\sim 6\sigma$) limits the robustness of size measurements, the visibility function (Figure **??**) for LH 850.02 is consistent with a compact point–source out to ∼120 kλ, from which we infer a maximum angular extent of $\lesssim$1 arcsec; similar to other SMGs detected by SMA at 890 μm (**???**) and others observed at mm wavelengths (**??**). At a redshift of $z \approx 3-3.5$, this corresponds to a physical scale for the rest-frame far-IR continuum of $\lesssim$8 kpc, consistent with a merger-driven starburst analogous to local ULIRGs (**????**, see also C. Wilson et al. 2008, in prep.; Iono et al. 2008, in prep.), and may be in conflict with cool, extended cirrus dust models (**??**) or a monolithic collapse scenario. Our constraints on size are only barely consis-

[1] There is a $\sim 2\sigma$ peak nearly coincident with LH850.02S; the 3σ upper limit is listed in Table 1. However we note that the primary detection accounts entirely for the SCUBA flux.

Figure 4. gas-to-dust ratios

tent with extended (∼1 arcsec) starbursts of the kind inferred from high-resolution radio imaging – though some sources are reported as compact even at ~ 0.2 arcsec resolution (**??**).

We can then use the observed submm–to–radio flux density ratio, coupled with photometric redshift and observed constraints on the physical scale of the rest–frame far–IR to infer some of the physical properties of the starburst. Figure 4 shows the submm-to-radio flux density ratio $S_{890\mu\rm m}/S_{1.4\rm GHz}$ for LH 850.02, as compared to the possible high-redshift SMGs from **?**, SMGs with optical redshifts from **?**, tracks for Arp 220, the models of **?** and the median radio-quiet quasar spectral energy distribution from **?**. The observed submm–to–radio flux density ratio of LH850.02N indicates a dust temperature of $\sim$ 60 K, which is consistent with the observed compactness of the submm emission (see **?**). Using the template SEDs of **?** for this best–fit dust temperature at the photometric redshift of $z \approx 3.3$, we find that the observed submm emission of $S_{890\mu m} = 12.8\,\rm mJy$ corresponds to a total IR luminosity of $L \sim 2\times10^{13}$ $\rm L_{\odot}$, which – assuming a **?** IMF – indicates a total SFR of $\sim 3000\ M_{\odot}$ yr^{-1} (**??**). Should even higher-resolution imaging place tighter limits on the physical scale of the submm emission in LH850.02N, such a confined, luminous starburst may have important physical consequences; Eddington arguments (e.g., **??**) suggest a minimal scale for such regions.

Finally, considering far–IR luminosity and compactness, the lack of detectable 24μm emission, and its observed submm–to–radio flux density ratio, we find that LH 850.02 appears to share many of the observed characteristics of other putative high-redshift SMGs (**????**). As discussed in more detail in **?**, the existence of such a population provides tight constraints on models of galaxy formation and evolution, and on dust production. In addition, it fuels speculation that the brightest SMGs may be the most distant (see also **?**) and suggests significant and rapid down-sizing (e.g., **?**) in the SMG population over a relatively short interval in cosmic time (see also **?**).

4 CONCLUSION

We present high-resolution 890-μm interferometric imaging of H1549

ACKNOWLEDGEMENTS

The SMA is a joint project between the Smithsonian Astrophysical Observatory and the Academia Sinica Institute of Astronomy and Astrophysics and is funded by the Smithsonian Institution and the Academia Sinica. This work is based in on observations made with the *Spitzer Space Telescope*, which is operated by the Jet Propulsion Laboratory, California Institute of Technology, under contract 1407, and data collected at Subaru Telescope, which is operated by the National Astronomical Observatory of Japan. The James Clerk Maxwell Telescope is operated by The Joint Astronomy Centre on behalf of the Science and Technology Facilities Council of the United Kingdom, the Netherlands Organisation for Scientific Research, and the National Research Council of Canada. IS acknowledges support from the Royal Society.